Research & Development

White Paper

WHP205

September 2011

A simple model of the UHF cross-polar terrestrial channel for DVB-NGH

Peter Moss, Tuck Yeen Poon and John Boyer

BRITISH BROADCASTING CORPORATION

White Paper WHP 205

A simple model of the UHF cross-polar terrestrial channel for DVB-NGH

Peter Moss, Tuck Yeen Poon and John Boyer

Abstract

The successor to the DVB-H broadcast handheld standard (DVB-NGH) is currently being defined by the DVB-TM-H working group. A key feature which would distinguish the new standard from the old is the likely inclusion of cross-polar transmission and reception for increased capacity and robustness through twin-antenna MIMO schemes. To enable simulations of the various proposals to be carried out, a channel sounding campaign took place in July 2010 in Helsinki, Finland, focussing on cross-polar UHF transmission and reception. A number of practical designs for antennas suitable for a handheld terminal were included in the trial and all test data was obtained via these devices. Following the campaign, analysis of the data has produced a simple model for both outdoor and indoor scenarios of the antenna-inclusive 2-by-2 channel.

This paper briefly describes the excitation signal and test arrangements before introducing the form of the channel model. Finally the actual parameters of the model which have resulted from the measurements are discussed and related to the likely observable behaviour of the NGH cross-polar signal.

Keywords

Channel model, Cross-polar, DVB-H , Handheld , NGH, UHF

This document is based on that originally published in the International Journal of Sensors, Wireless communications and Control vol. 1 no. 1 June 2011 ISSN:2210-3279

White Papers are distributed freely on request.

Authorisation of the Chief Scientist or General Manager is required for publication.

White Paper WHP 205

A simple model of the UHF cross-polar terrestrial channel for DVB-NGH

Peter Moss, Tuck Yeen Poon and John Boyer

List of Abbreviations

BBC	British Broadcasting Corporation
DVB-T	Digital Video Broadcasting (Terrestrial)
DVB-T2	Digital Video Broadcasting (Terrestrial), second generation
DVB-H	Digital Video Broadcasting (Handheld)
DVB-NGH	Digital Video Broadcasting (Next Generation Handheld)
EB	Elektrobit Corporation
LOS/NLOS	Line of sight/ Non line of sight
MEDS	Method of Exact Doppler Spread
MIMO	Multiple-Input-Multiple-Output
MISO	Multiple-Input-Single-Output
OFDM	Orthogonal Frequency Division Multiplex
PDP	Power delay profile
PSD	Power spectral density
SFN	Single Frequency Network
SISO	Single-Input-Single-Output
TUAS	Turku University of Allied Sciences
UHF	Ultra High Frequency
XPD	Cross-polar discrimination
YLE	Yleisradio Oy

1 Introduction

Following the introduction of DVB-T2 (Digital Video Broadcasting – Terrestrial) as a second-generation system for terrestrial broadcasting, work is currently underway within the DVB organisation to define a successor to the handheld DVB-H standard. A key feature which would distinguish the new standard from the old is the likely inclusion of cross-polar transmission and reception for increased capacity and robustness through twin-antenna MIMO schemes. In order to appraise and compare candidate schemes in simulation a realistic measurement-based channel model was required and to this end a channel sounding campaign took place in July 2010 in Helsinki, Finland, focussing on cross-polar UHF transmission and reception. A number of practical designs for antennas suitable for a handheld terminal were included in the trial and all test data was obtained via these devices. Following the campaign, analysis of the data has produced a simple model for both outdoor and indoor scenarios of the antenna-inclusive 2-by-2 channel.

This paper briefly describes the excitation signal and test arrangements before introducing the form of the channel model. Finally the actual parameters of the model which have resulted from the measurements are discussed and related to the observable behaviour of the NGH cross-polar signal.

The model describes fast fading as seen during antenna displacements of up to 50m rather than slow fading caused by shadowing or large scale path loss. Two variants are provided, defining outdoor pedestrian and indoor reception respectively. A 4 x 2 model or SFN (Single Frequency Network) model may be derived from two uncorrelated 2 x 2 models of the type described, the excess delays of one model being increased to be close to the defined system tolerance of the system under test (for instance to 90% of the guard interval).

2 The channel measurement system

2.1 Overview

The channel sounding campaign was carried out in Helsinki, Finland, in collaboration with Digita Oy, Elektrobit (EB), Nokia, Amphenol, Turku University of Applied Sciences and Tampere University. The sounding data was transmitted from a 146 meter high TV tower in Pasila, situated to the north of Helsinki city centre.

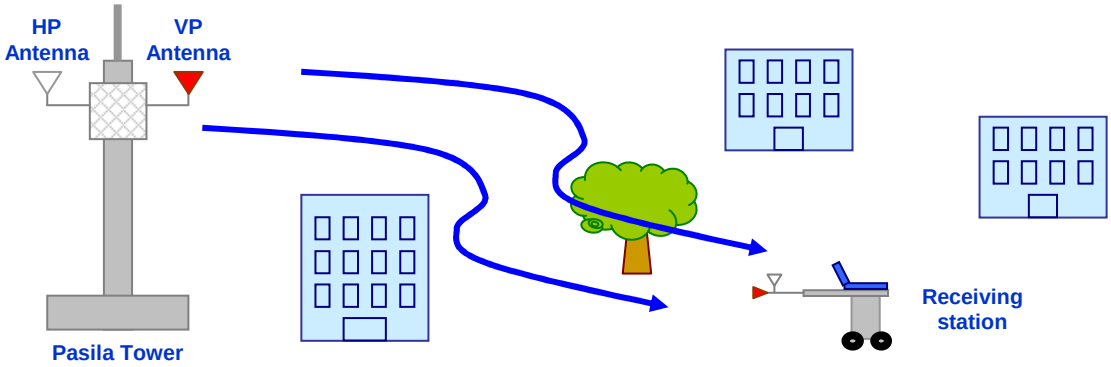

Figure 1: Channel sounding in Helsinki

Two separate transmit antennas; horizontally-polarised (HP) and vertically-polarised (VP), were fixed on the transmitting tower and a series of cross-polarised patch antennas were mounted on the mobile receiving station to create a representative 2-by-2 MIMO system.

2.2 Block diagram

The block diagram of the transmitter and receiver is shown in Figure 2. The 'Inv' block on the transmit side inverts the signal on every other OFDM symbol. Each transmit-path (Tx0/Tx1) feeds into a power amplifier before it is connected to the HP and VP antenna respectively.

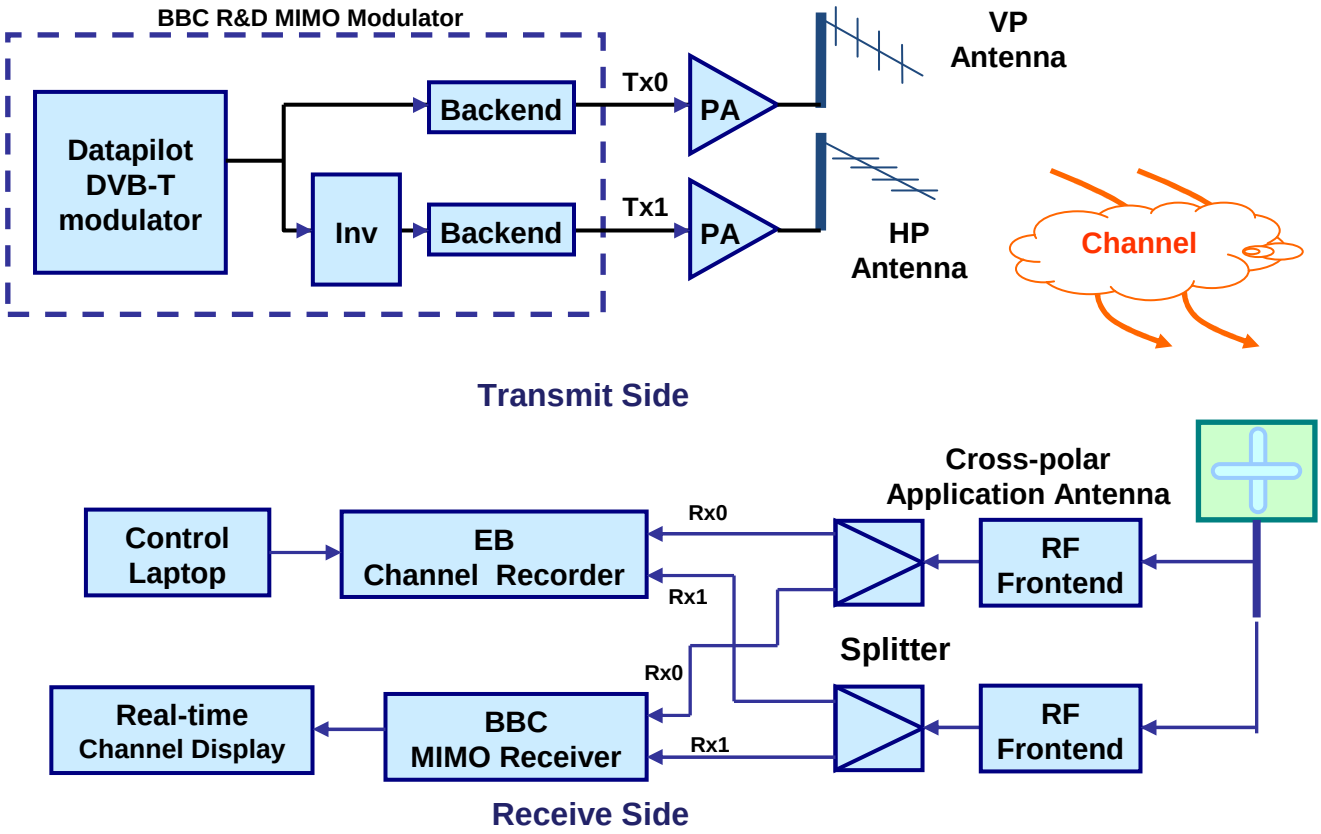

Figure 2: Block diagram of transmit and receive side

On the receiving side, the portable receiver consisted of the cross-polarised application antennas, channel recorder and the real-time channel display which obtained its data from a hardware MIMO receiver. The channel recorder is controlled using a laptop computer with proprietary software.

2.3 Signal specification

The DVB-T OFDM-based modulated signal which was used to sound the channel is defined in appendix A.

2.4 Campaign realisation

2.4.1 Transmitter

The transmitter (YLE Transmission Tower) used during this channel sounding campaign was located in Pasila, in the north of Helsinki city, and it is 146 metres high. Two standard UHF antenna panels, one HP and the other VP, were used and these are shown in Figure 3 along with the transmitting tower.

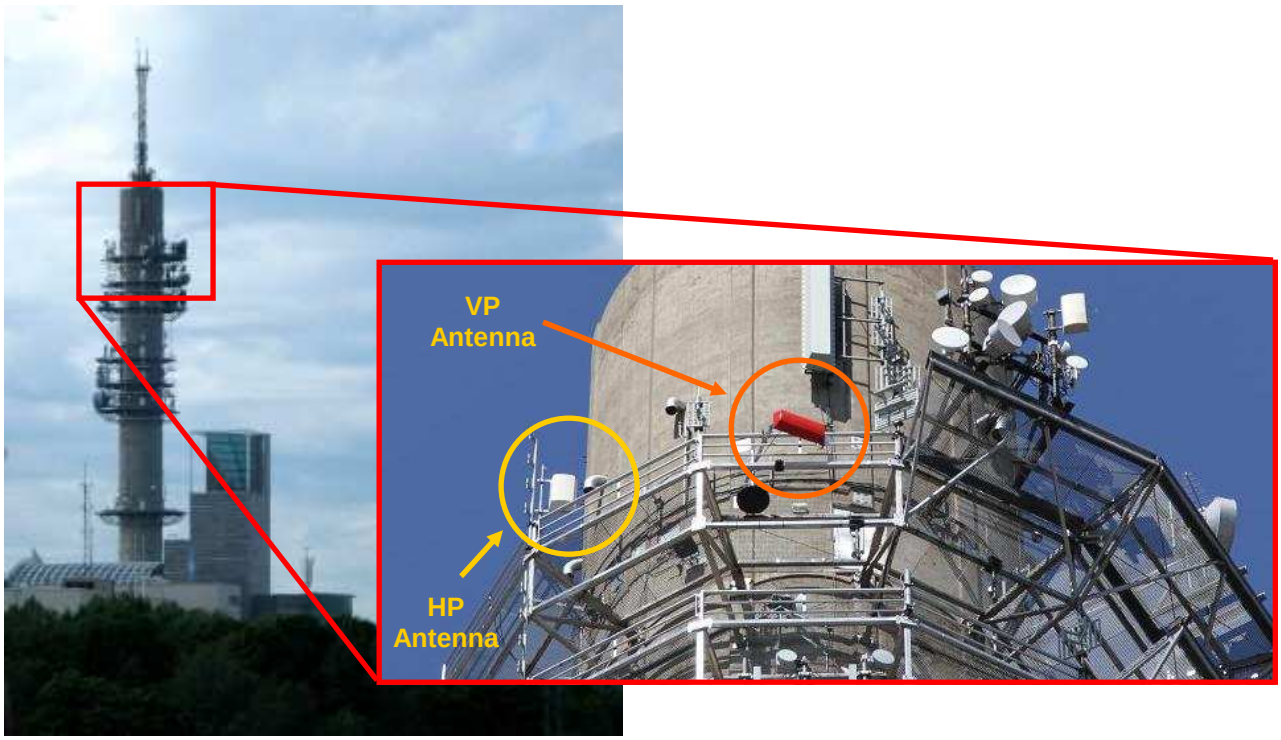

Figure 3: YLE Transmission Tower at Pasila & the transmitting antennas

The transmit antennas were standard horizontally polarised UHF panels. One of the panels was rotated through 90º to act as a vertically polarised transmit antenna. The panels comprised 4 stacked dipoles this means that the beamwidth of the vertical radiation pattern was considerably narrower than the horizontal radiation pattern. This restricted beamwidth meant that the VP antenna was unable to cover all the measurement locations. Therefore, the VP antenna employed a mechanism to steer it ensuring that the sounding location has similar field strength levels for both polarisations.

The MIMO modulator used for this sounding was connected to two power amplifiers inside the transmitting tower as shown in Figure 4.

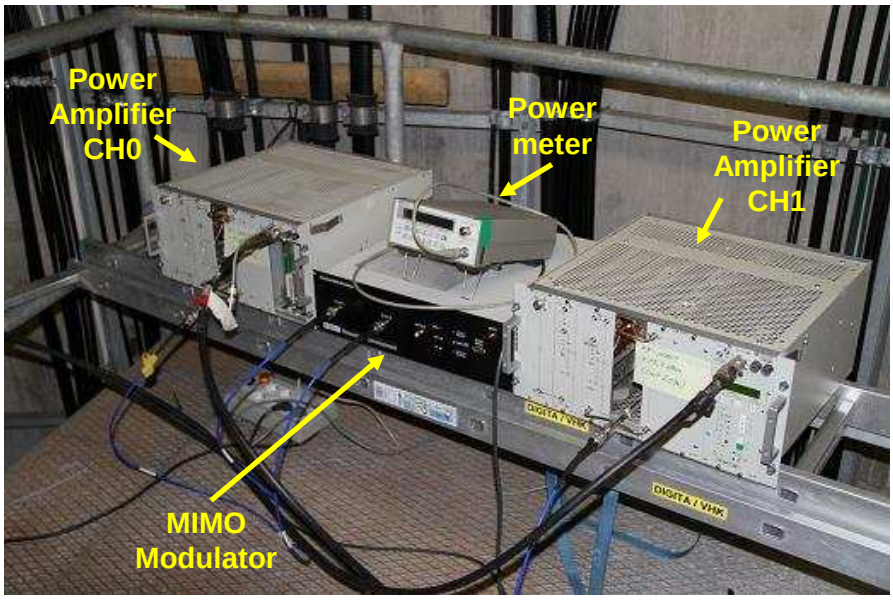

Figure 4: BBC MIMO Modulator and Power Amplifiers

The output of the power amplifiers was measured with a power meter via an attenuator to ensure that there was no power imbalance between the two power amplifiers that fed into the transmit antenna. Note; that this did not take into account any losses in cables between the amplifiers and the antennas, as this was not readily accessible.

2.4.2 Receiver

The portable receiving station was constructed as shown in Figure 5 and consisted of the EB channel recorder (connected to the control laptop), BBC MIMO receiver with real-time channel display, cross-polar application antenna and batteries to power up all the equipment. All these were mounted on a push trolley and the application antenna was mounted on an 'extended-arm' to minimise interference from the equipment. The antenna was about 1.5 meters above ground.

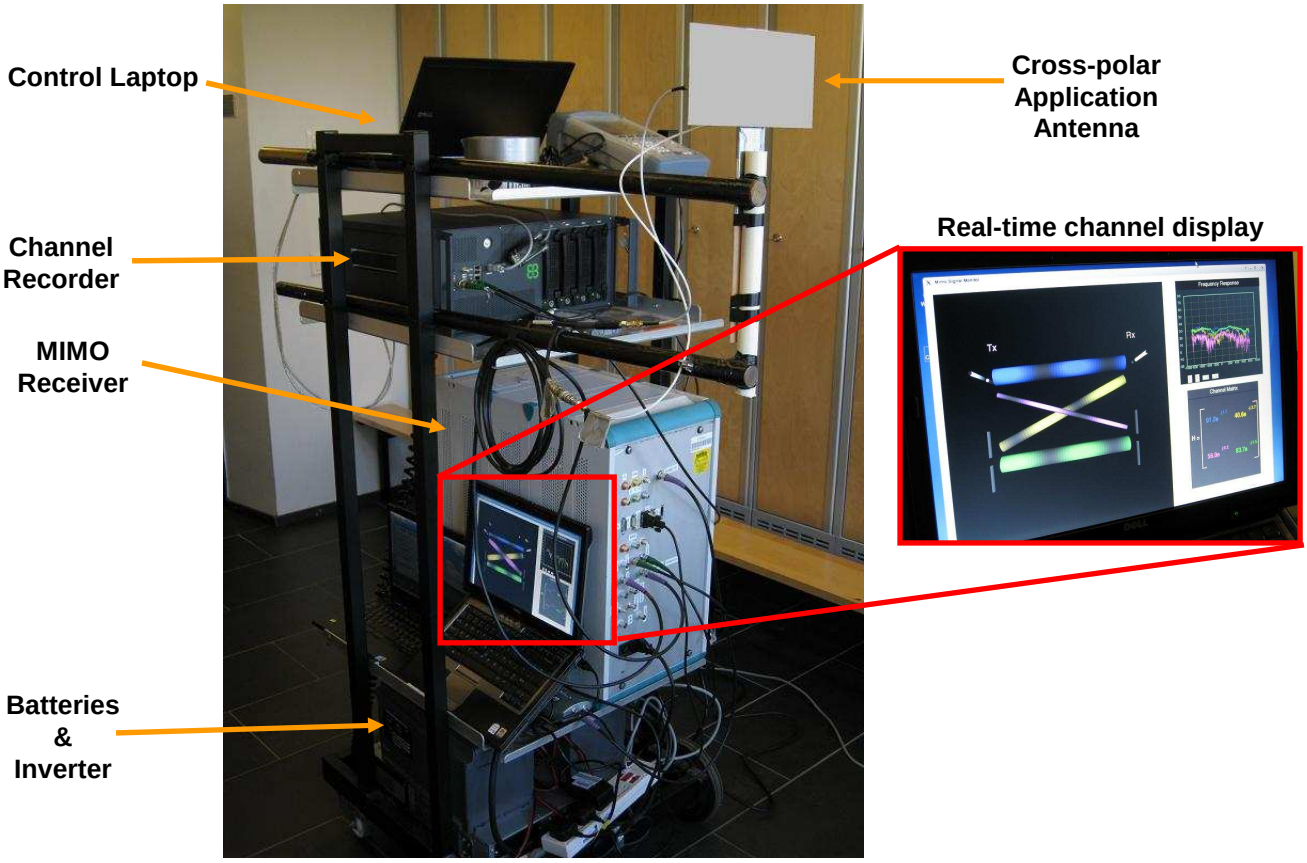

Figure 5: Portable receiving station

The real-time channel display was very useful to give an instant feedback on the channel response and to ensure the integrity of the captured data.

2.4.3 Measurement Campaign

The channel sounding was done at five different locations covering indoor and outdoor scenarios, and over 100 measurements were recorded with 280GB of data. Five cross-polar application antennas designed by various partners were used in this campaign with the intention that the channel model extracted from this campaign is representative of a practical antenna.

The locations where the measurements were taken are shown in Figure 6 along with the location of the YLE Transmission Tower in Pasila.

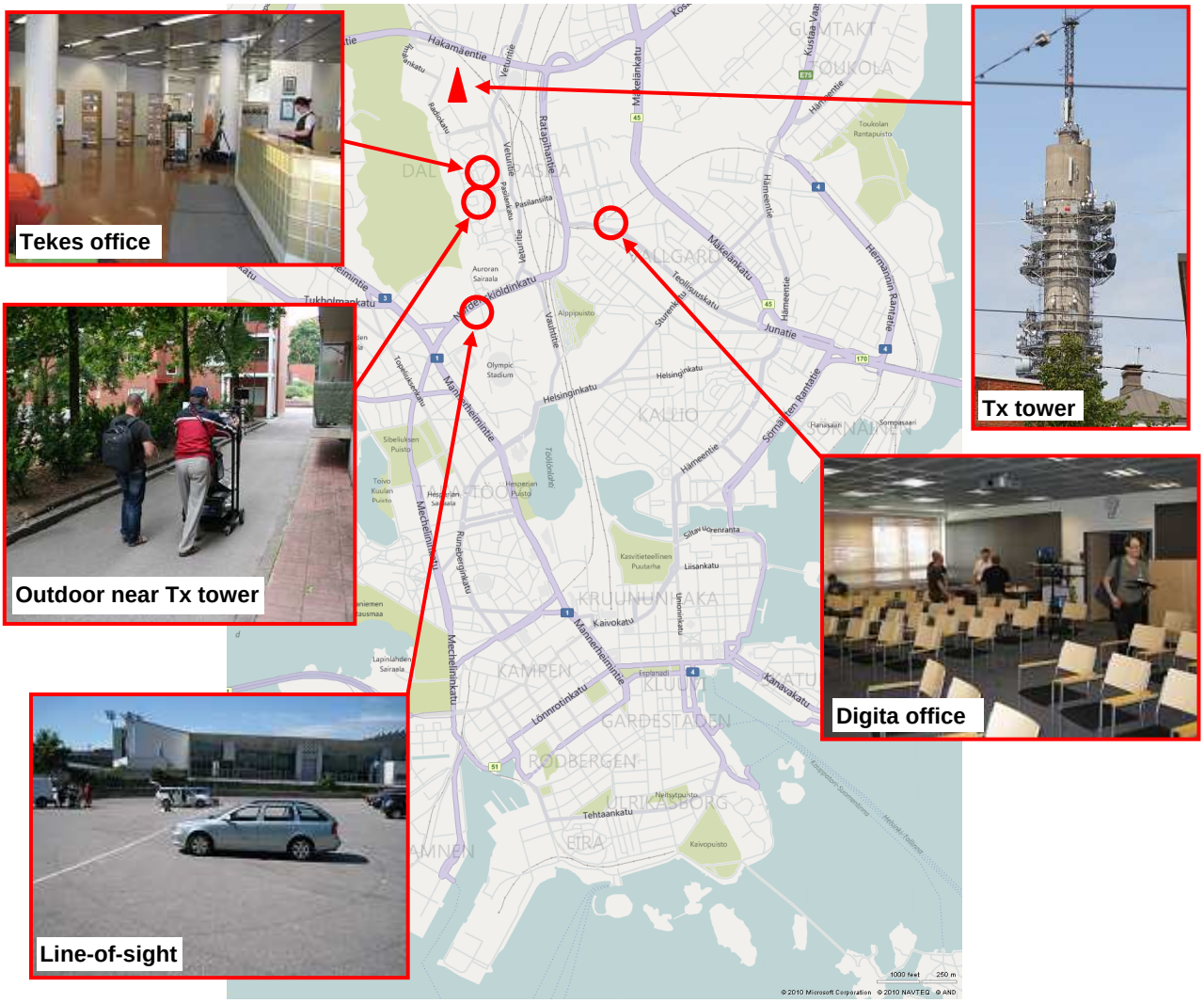

Figure 6: Locations where measurements were taken

The type of location and measurement was carefully planned to capture as many scenarios as possible. The indoor capture scenarios include measurements along a corridor, inside a conference room, at reception area and inside an office while the outdoor scenarios include line-of-sight (LOS) and non-line-of-sight (NLOS) environment.

Every care was taken during the trial and calibration runs were done throughout the campaign to ensure all equipment on the portable receiving station was working.

Figure 7: Outdoor measurement

Figure 8: Indoor measurement

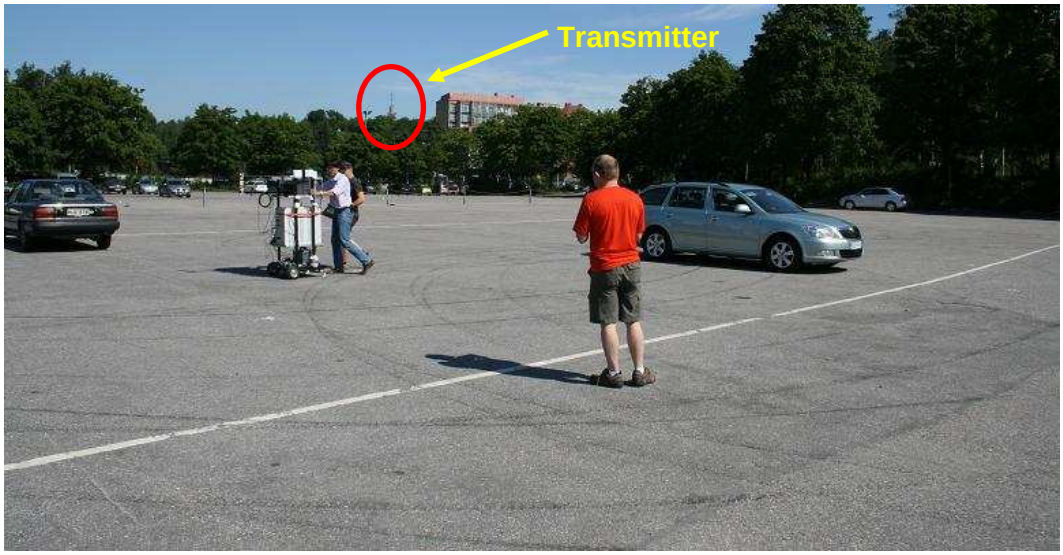

Figure 9: Outdoor line-of-sight measurement

3 The channel model

3.1 General approach

The aim is to provide a time-domain model of paths shown as $h_{11}, h_{12}, h_{21}, h_{22}$ in the figure below, where Tx1 and Tx2 represent twin antenna elements at a terrestrial transmitter site and Rx1 and Rx2 the two elements of the MIMO receive antenna. It is important to note that the model is antenna-inclusive so it is intended to represent the full transmitter output to receive terminal input path.

The model describes fast fading as seen during antenna displacements of up to 50m rather than slow fading caused by shadowing or large scale path loss. This allows receiver algorithm testing to be carried out satisfactorily as the path/loss shadowing is implicitly included in the choice of test signal-to-noise ratio.

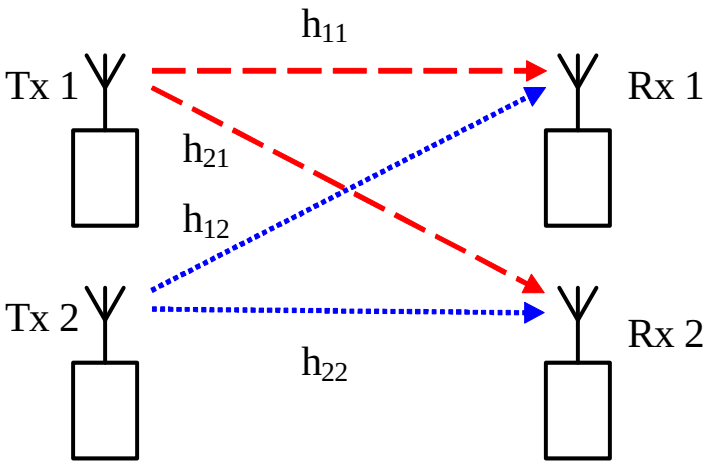

Figure 10 - 2-by-2 MIMO system

An 8-tap model of the propagation paths was proposed, to include the contribution of a 'representative' antenna, with each parameter based on an average or typical behaviour of those made available for the trial. The model has two variants, 'indoor' and 'outdoor', customised to represent those scenarios by suitable choices of parameters.

The delays and relative powers of the paths are tabulated below in paragraph 3.4

3.2 Mathematical form of the model

A simplifying assumption underpinning the model is symmetry of the Horizontal/Vertical fading components. This was largely confirmed by observation, although differences in the transmit antenna H/V patterns made it difficult to establish the precise balance. As a working assumption for modelling and simulation the approximation was considered adequate. Similarly, the cross-polar coupling is taken as symmetrical.

The channel model for both indoor and outdoor variants has the common form below:

$$\mathbf{vec}(\mathbf{H}^T(t,\boldsymbol{\tau})) = \mathbf{L}_1(t)\boldsymbol{\delta}(\boldsymbol{\tau}-\boldsymbol{\tau}_1) + \sum_{j=1}^{8}\mathbf{R}_j^{1/2}\mathbf{x}_j(t)\boldsymbol{\delta}(\boldsymbol{\tau}-\boldsymbol{\tau}_j) \quad \ldots\ldots\ldots\ldots\ldots\ldots\ldots\ldots (7)$$

where t is the time index, τ the delay-time and τ_j the delay-time position of the j^{th} tap (as tabulated below in tables 1 and 2).

$$\mathbf{vec}(\mathbf{H}^T(t,\tau)) = \begin{pmatrix} h_{11}(t,\tau) \\ h_{12}(t,\tau) \\ h_{21}(t,\tau) \\ h_{22}(t,\tau) \end{pmatrix} \ldots\ldots (8)$$

A 2x2 time-variant channel matrix **H** is hence:

$$\mathbf{H}(t,\tau)=\begin{bmatrix} h_{11}(t,\tau) & h_{12}(t,\tau) \\ h_{21}(t,\tau) & h_{22}(t,\tau) \end{bmatrix}$$

The line-of-sight term is given by

$$\mathbf{L}_1(t)=\sqrt{\frac{K_1P_1}{1+K_1}}\begin{pmatrix} \exp(j\theta_{11}) \\ w\exp(j\theta_{12}) \\ w\exp(j\theta_{21}) \\ \exp(j\theta_{22}) \end{pmatrix}\ldots\ldots(9)$$ where K_1 is the tap 1 Ricean K-factor.

If the tap is pure line-of-sight (LOS), the expression reduces to

$$\mathbf{L}_1(t)=\sqrt{P_1}\begin{pmatrix} \exp(j\theta_{11}) \\ w\exp(j\theta_{12}) \\ w\exp(j\theta_{21}) \\ \exp(j\theta_{22}) \end{pmatrix}\ldots\ldots(9A)$$

$\mathbf{R}_j$ is the 4-by-4 covariance matrix of the 4-element coefficient vector $\mathbf{c}_j=\mathbf{R}_j^{1/2}\mathbf{x}_j(t)$ at the j^{th} tap, ordered as (8). The terms $\mathbf{x}_j$ are (distinct) random vectors for each j with i.i.d. complex Gaussian components of unit variance. They are time-varying with a power spectral density (PSD) in accordance with paragraph 3.7.

$\mathbf{L_1}$ defines the tap 1 line-of-sight LOS terms; it has uniformly distributed random phases θ_{nm} in the interval [0, 2π).

P_j is the total power of the j^{th} tap weight associated with terms h_{11}, h_{22}, i.e. $P_1=\mathbf{L}_1^2+|\mathbf{c}_1(1)|^2=\mathbf{L}_1^2+|\mathbf{c}_1(4)|^2$ and $P_j=|\mathbf{c}_j(1)|^2=|\mathbf{c}_j(4)|^2\ldots\ldots j\neq 1$.

The coefficient *w* adjusts the power level appropriately for the terms h_{12}, h_{21}.
For the indoor model, *w*=0.562 (2.5dB); for the outdoor model *w*=0.25 (6dB).

Since tap 1 has both a LOS and Rayleigh component, the latter has a power level $\frac{1}{1+K_1}$ of the tabulated tap power P_1. See paragraph 3.5.

The required square root of $\mathbf{R}_j$ satisfies $\mathbf{R}_j=\mathbf{R}_j^{1/2}\mathbf{R}_j^{H/2}$ and can be obtained from the Cholesky decomposition of $\mathbf{R}_j$.

The tap covariance matrix is common to taps 2-8 and the Rayleigh part of tap 1 within each model variant. See paragraph 3.6 below.

3.3 Additional antenna rotation and asymmetry terms

In deriving the antenna-specific data from which the model parameters were derived, the raw data was rotated by up to ±40º to find the angle which maximised the cross-polar discrimination. This was to correct for both physical mounting differences and antenna axis differences with respect to the casing. It also ensured averaging across antennas retained legitimacy in terms of cross-polar discrimination.

However in practice this 'ideal' alignment may not be representative and so a further rotation matrix **W**, with angle Ω chosen from the set {-45 º, 0 º, +45 º} is recommended with the angle fixed for a particular simulation run.

In addition, an asymmetry matrix **Γ** is included to model observed H/V asymmetries which persist over many contiguous channel realisations (~10m). **Γ** is also fixed for a particular simulation run and takes values from the set

$$\left\{\begin{bmatrix} 1.1074 & 0 \\ 0 & 0.8796 \end{bmatrix} \begin{bmatrix} 1 & 0 \\ 0 & 1 \end{bmatrix} \begin{bmatrix} 0.8796 & 0 \\ 0 & 1.1074 \end{bmatrix}\right\}.$$

The resulting channel matrix $\mathbf{H_c}(t,\tau)$ is hence derived from **H** as follows:

$$\mathbf{H}_{\mathbf{c}}(t,\boldsymbol{\tau}) = \mathbf{WH}(t,\boldsymbol{\tau})\boldsymbol{\Gamma} = \begin{bmatrix} \cos\Omega & -\sin\Omega \\ \sin\Omega & \cos\Omega \end{bmatrix} \begin{bmatrix} h_{11}(t,\boldsymbol{\tau}) & h_{12}(t,\boldsymbol{\tau}) \\ h_{21}(t,\boldsymbol{\tau}) & h_{22}(t,\boldsymbol{\tau}) \end{bmatrix} \begin{bmatrix} \Gamma_{11} & 0 \\ 0 & \Gamma_{22} \end{bmatrix} \quad (10)$$

3.4 Tap values

The tap values P_j are set so as to model the power delay profile (PDP) of the channel. Two sets of tap values were derived from the data, corresponding to the indoor and outdoor scenarios. These are tabulated below

Table 1: Tap values – indoor model

Tap number *j*	**Excess delay (μs)**	$\boldsymbol{P_j}$ (h_{11}, h_{22})	$\boldsymbol{wP_j}$ (h_{12}, h_{21})
		All terms dB	*All terms dB*
1	0	-6.0	-8.5
2	0.1094	-8.0	-10.5
3	0.2188	-10.0	-12.5
4	0.6094	-11.0	-13.5
5	1.109	-16.0	-18.5
6	2.109	-20.0	-22.5
7	4.109	-20.0	-22.5
8	8.109	-26.0	-28.5

Table 2: Tap values – outdoor model

Tap number j	**Excess delay (μs)**	$\boldsymbol{P}_j$ (h_{11}, h_{22})	$\boldsymbol{wP}_j$ (h_{12}, h_{21})
		All terms dB	*All terms dB*
1	0	-4.0	-10.0
2	0.1094	-7.5	-13.5
3	0.2188	-9.5	-15.5
4	0.6094	-11.0	-17.0
5	1.109	-15.0	-21.0
6	2.109	-26.0	-32.0
7	4.109	-30.0	-36.0
8	8.109	-30.0	-36.0

3.5 Ricean K-factor

The K-factor of each matrix element was estimated using the method of moments [2], which first evaluates the second and fourth moments of the frequency response data along the *t*-axis[1]. From this, the K-factor of an assumed underlying Ricean distribution may be deduced. The K-factors of the model are tabulated below

Table 3: Ricean K-factors

Model	**First tap**	**Overall**
Indoor	1.0	0.2
Outdoor	LOS only, K= ∞	1.0

3.6 Tap correlation matrices

The tap correlation matrix for the indoor channel is given by (except for tap 1):

$$\mathbf{R}_j = P_j \begin{pmatrix} 1.00 & 0.15 & 0.10 & 0.15 \\ 0.15 & 0.56 & 0.06 & 0.04 \\ 0.10 & 0.06 & 0.56 & 0.15 \\ 0.15 & 0.04 & 0.15 & 1.00 \end{pmatrix} \qquad j \in \{2 \ldots 8\} \quad \ldots\ldots\ldots\ldots\ldots\ldots\ldots\ldots\ldots\ldots\ldots\ldots (11)$$

For tap 1, we have

[1] i.e. we examine the evolution in time of each frequency bin and assign a K to each, from which an overall K is deduced.

$$\mathbf{R}_1 = \frac{1}{1+K_1} P_1 \begin{pmatrix} 1.00 & 0.15 & 0.10 & 0.15 \\ 0.15 & 0.56 & 0.06 & 0.04 \\ 0.10 & 0.06 & 0.56 & 0.15 \\ 0.15 & 0.04 & 0.15 & 1.00 \end{pmatrix} \quad \ldots\ldots\ldots\ldots\ldots\ldots\ldots\ldots\ldots\ldots\ldots\ldots (12)$$

The tap correlation matrix for the outdoor channel is given by (except for tap 1):

$$\mathbf{R}_j = P_j \begin{pmatrix} 1.00 & 0.06 & 0.06 & 0.05 \\ 0.06 & 0.25 & 0.03 & 0.05 \\ 0.06 & 0.03 & 0.25 & 0.06 \\ 0.05 & 0.05 & 0.06 & 1.00 \end{pmatrix} \qquad j \in \{2 \ldots 8\} \ldots\ldots\ldots\ldots\ldots\ldots\ldots\ldots\ldots\ldots\ldots\ldots (13)$$

For tap 1, the energy is pure LOS, so there is no Rayleigh part to the fading. Hence $\mathbf{R}_1=[0]_{4x4}$

3.7 Doppler spectrum

3.7.1 Overview

Whilst the experimental methodology of pushing a trolley at approximately constant speed was sufficient to produce an indicative spectrum, it was clearly not sufficiently accurate to produce quantitative results. Because of this, it was decided at the outset to use a 'Classical' power spectral density (PSD) as a basis of the Rayleigh fading taps. This PSD (also known as Jakes Doppler spectrum) is given by

$$S(f, f_d) = \frac{1}{\pi f_d \sqrt{1-(f/f_d)^2}} \ldots\ldots\ldots\ldots |f| \le f_d \ldots\ldots\ldots\ldots\ldots\ldots\ldots\ldots\ldots\ldots (14)$$

and is zero elsewhere.

f_d is a parameter controlling the maximum Doppler width. It is chosen to be proportional to an assumed vehicle speed. The form of this PSD is illustrated in figure 11 (with arbitrary scales), which is a plot from a simulation based on the Method of Exact Doppler Spread (MEDS), to be outlined in appendix B.

Figure 11:Jakes spectrum from MEDS model simulation

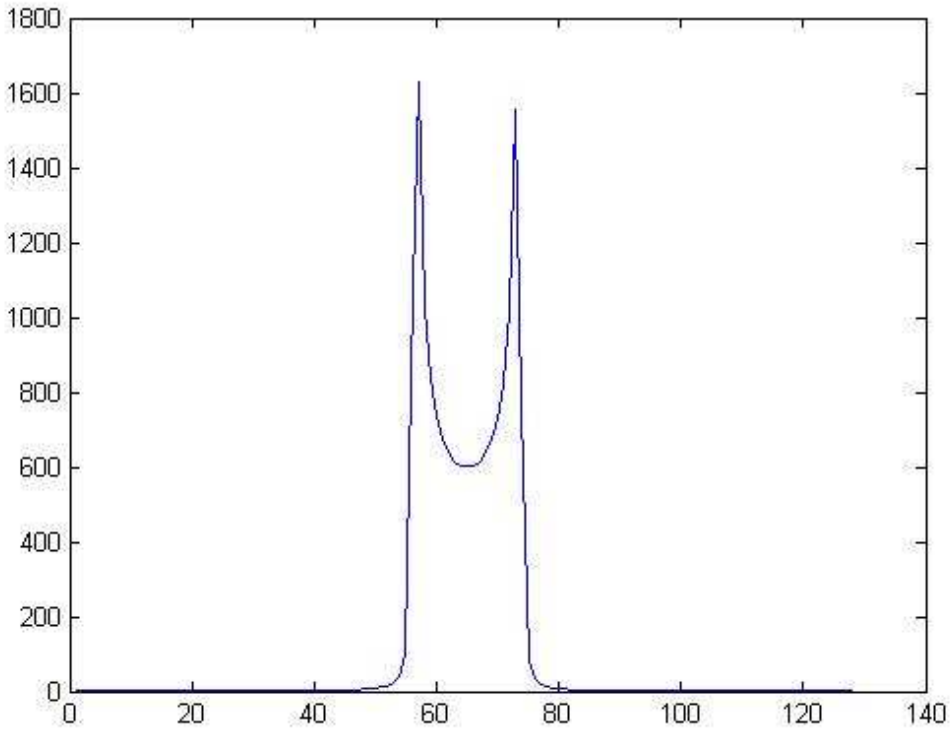

In this model, the Jakes spectrum is specified to be used at a particular tap in conjunction with a fixed frequency offset (pure Doppler) proportional to f_d. Table 4 below specifies the spectra of each tap.

Table 4: Tap Doppler Spectra

Tap number, *p*	**Spectrum**
1 (Indoor model NLOS component only)	$S(f, f_d)$
2	$S\left(f - \frac{3f_d}{4}, \frac{f_d}{4}\right)$
3	$S\left(f - \frac{3f_d}{4}, \frac{f_d}{4}\right)$
4	$S\left(f + \frac{3f_d}{4}, \frac{f_d}{4}\right)$
5	$S\left(f + \frac{3f_d}{4}, \frac{f_d}{4}\right)$
6	$S\left(f + \frac{3f_d}{4}, \frac{f_d}{4}\right)$
7	$S\left(f + \frac{3f_d}{4}, \frac{f_d}{4}\right)$
8	$S\left(f + \frac{3f_d}{4}, \frac{f_d}{4}\right)$

3.7.2 Choice of Doppler width parameter f_d

To represent portable reception, both indoor and outdoor, receive terminal speeds of 0km/h and 3km/h are specified. At 600MHz carrier frequency, the latter corresponds to 1.667Hz Doppler width f_d. For the 0km/h case, see 3.7.3 below.

3.7.3 Stationary channels ('snapshots')

If we simulate a time-invariant channel, i.e. $f_d = 0$, the Doppler shift for the LOS components and the Doppler spreads for the NLOS components are not modelled by the procedures described above. Instead, a number of independent realizations ('snapshots') should be generated in which the vectors $\mathbf{x}_j$ remain (distinct) for each j retain the the prescribed intra-tap correlation properties, but are not time-varying, so the MEDS procedure is not invoked.

3.8 Mobile vehicular outdoor model

For the mobile case, the outdoor model is used but with f_d = 33.3Hz and 167Hz Doppler half-width.

This corresponds to 60km/h and 300km/h at 600MHz.

3.9 4 x 2 model

A pair of uncorrelated 2 x 2 models can be used to represent a 4x2 transmission from two cross-polar towers. A time offset between them can also be introduced to represent different receiver positions with respect to each tower, together with a level offset characteristic of the scenario under test.

4 SISO, MISO and SIMO systems

Appropriate transmission paths of the MIMO model may be selected to provide SISO (single-input-single output), MISO (multiple-input-single-output) and SIMO (single input multiple output) models. For SISO, this amounts to using h_{11} or h_{22} (which have identical statistics); for SIMO h_{11} and h_{21}; and for MISO h_{11} and h_{12}. Of course it must be remembered that the model is appropriate only for the cross-polar transmission/reception case, so the MISO variant has limited practical application. The SIMO model does, however, represent a realistic case of dual-polarised reception of single-polarised transmission; for instance with rotation-insensitive handset antenna designs.

5 Conclusions

A model of the UHF cross-polar channel primarily intended for transmitter/receiver algorithm testing within the DVB-NGH project has been presented. An outline of the measurement system and measurement location has been included, together with a description of the form of the model and key parameters characterising the indoor and outdoor scenarios.

6 Acknowledgements

The authors would like to thank the BBC for permission to publish this paper, and their DVB-NGH colleagues for their advice and contributions to this work. Particular thanks go to Joerg Robert of the Technical University of Braunschweig for assisting with the post-processing, Pekka Talmoloa of Nokia for facilitating the field trial, the Elektrobit Corporation of Finland for providing the signal capture system, Digita of Finland for providing the transmission facility and of course the various providers of the application antennas.

7 References

[1] M. Patzold, U. Killat, F. Laue, and Y. Li, “On the statistical properties of deterministic simulation models for mobile fading channels” IEEETrans. Veh. Technol., /vol. VT-47, no. 1, pp. 254-269, Feb. 1998.
[2] "On the estimation of the K parameter for the Rice fading distribution "Ali Abdi, Student Member, IEEE, Cihan Tepedelenlioglu, Student Member, IEEE, Mostafa Kaveh, Fellow, IEEE, and Georgios Giannakis, Fellow, IEEE Dept. of Elec. and Comp. Eng., University of Minnesota
[3] ETSI EN 300 744 V1.4.1 (2001-01) : Digital Video Broadcasting (DVB); Framing structure, channel coding and modulation for digital terrestrial television

Appendix A: Channel Sounding signal specification

1 Technical summary

The proposed signal is based the OFDM format of DVB-T. This signal is defined in [3] and features a 1-in-12 pilot structure intended for channel estimation. The first transmitter radiates DVB-T scattered pilots, continual pilots and TPS pilots exactly as defined in [3]. Since 2-transmitter MIMO channel measurement is required, modifications to the signal for the second transmitter are necessary. These are as follows: on every other OFDM symbol, the sign of the scattered pilots is reversed (i.e. the pilot is inverted) with respect to that defined in [3]. In addition, continual pilots which lie on carriers which at times coincide with an inverted pilot are permanently inverted to allow consistency when they are indeed coincident.

TPS data is arbitrary as it is not anticipated it will be used in the channel measurement applications.

The data cells are assigned fixed BPSK data obtained from the DVB-T reference sequence of [3] para. 4.5.2.

2 Signal definition

2.1 OFDM frame structure

OFDM frame structure shall be as reference [3] paragraph 4.4 with the following changes/exceptions:

2k mode only
8MHz channel only

2.2 Reference signals

2.2.1 Location of scattered pilots

Reference information, taken from the reference sequence of [3] para. 4.5.2, is transmitted in scattered pilot cells in every symbol.

Scattered pilot cells are always transmitted at the "boosted" power level of 16/9 relative to data bearing carriers. Thus the corresponding modulation is given by:

$$\mathrm{Re}\{c_{m,l,k}\} = \frac{4}{3} \times 2\left(\frac{1}{2} - w_k\right)$$

$$\mathrm{Im}\{c_{m,l,k}\} = 0$$

where m is the frame index, *k* is the frequency index of the carriers and *l* is the time index of the symbols.

For the symbol of index *l* (*l* ranging from 0 to 67), carriers for which index *k* belongs to the subset

$k = K_{min} + 3 \times (l \bmod 4) + 12p$ (p integer, $p \geq 0$, *k* in range $[K_{min}; K_{max}]$) are scattered pilots.

The pilot insertion pattern is shown in figure 11 of para [3] 4.5.3.

2.2.2 Location and modulation of continual pilots

In addition to the scattered pilots, 45 locations for continual[2] pilots are defined in [3] para. 4.5.4 for 2k mode.

All continual pilots are modulated according to the reference sequence, see ref.[3] para. 4.5.2.

The continual pilots are transmitted at "boosted" power level.

Thus the corresponding modulation is given by, on transmitter 1 of 2:

$$\mathrm{Re}\{c_{m,l,k}\} = \frac{4}{3} \times 2\left(\frac{1}{2} - w_k\right)$$

$$\mathrm{Im}\{c_{m,l,k}\} = 0$$

2.2.3 Modification to pilots on transmitter 2

Transmitter 2 has scattered pilots inverted every other OFDM symbol to allow for MIMO channel measurement. Continual pilots falling on scattered-pilot-bearing carriers are inverted compared to transmitter 1 if the coincident scattered pilot is inverted; continual pilots without this property are not inverted.

Scattered pilots on transmitter 2:

$$\mathrm{Re}\{c_{m,l,k}\} = \frac{4}{3} \times (-1)^l \times 2\left(\frac{1}{2} - w_k\right)$$ (symbol no. *l* in the range 0…67)

$$\mathrm{Im}\{c_{m,l,k}\} = 0$$

Continual pilots on transmitter 2:

[2] i.e. occurring on all symbols

$$\mathrm{Re}\{c_{m,l,k}\} = \frac{4}{3} \times (-1)^l \times 2\left(\frac{1}{2} - w_k\right) \text{ if } k \bmod 3 = 0$$

$$\mathrm{Re}\{c_{m,l,k}\} = \frac{4}{3} \times 2\left(\frac{1}{2} - w_k\right) \text{ otherwise}$$

$$\mathrm{Im}\{c_{m,l,k}\} = 0$$

2.2.4 Amplitudes of all reference information

Reference [3] para 4.5.5 shall apply.

2.3 TPS pilots

This is defined in accordance with [3] para. 4.6, 2k mode, but may have arbitrary information in s_0-s_{67}.

2.4 Data carriers

2.4.1 Location and modulation of the data carriers

The v^{th} data carrier associated with the l^{th} symbol of the m^{th} transmission frame is denoted here by $c^{(n)}{}_{m,l,v}$. The set of data carriers is the complement of the set of reference and TPS carriers, and we shall index it with v in the range (0….1511). The transmitter index is n, taking the value 1 or 2.

Transmitter 1:

Data carriers $c^{(1)}_{m,l,v}$ depend only on the indices v and l and are given by

$$\mathrm{Re}\{c^{(1)}_{m,l,v}\} = 2\left(\frac{1}{2} - d_{v,l}\right) \text{ for } v \in \{0 \ldots 1511\} \text{ and } l \in \{0 \ldots 67\}$$

$$\mathrm{Im}\{c^{(1)}{}_{m,l,v}\} = 0$$

with $d_{v,l}$ as specified in the following section 2.4.2

Transmitter 2:

Data carriers $c^{(2)}_{m,l,v}$ depend only on the indices *v* and *l* and are given by

$$\mathrm{Re}\left\{c^{(2)}_{m,l,v}\right\} = (-1)^l \times 2\left(\frac{1}{2} - d_{v,l}\right) \text{ for } v \in \{0\ldots1511\} \text{ and } l \in \{0...67\}$$

$$\mathrm{Im}\left\{c^{(2)}{}_{m,l,v}\right\} = 0$$

with $d_{v,l}$ as specified in the following section 2.4.2

2.4.2 PRBS sequence of the data carriers

The data carriers are modulated according to a different PRBS sequence, $d_{v,l}$, corresponding to their respective data carrier index *v and the symbol index l.* This PRBS sequence with its initialisation sequence is shown in figure 12.

Figure 12: Initialisation sequence

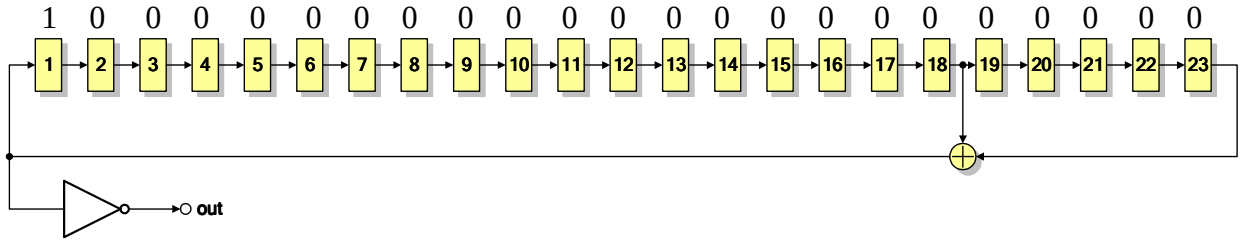

The PRBS is initialised so that the first output bit from the PRBS coincides with the first active carrier (data or signalling) of the first OFDM symbol in the frame, i.e. *l*=0. Subsequent bits from the sequence are mapped in order to the active carriers in the remaining symbols in the frame *l*=1 to *l*=67. However if the carrier is not a data carrier, the PRBS output is discarded. In this way, within the l^{th} symbol, 1705 bits are generated by the PRBS but only 1512 are used corresponding to *v* in the range 0…1511.

So if the sequence is u_m with $m \in 0\ldots(1705*68)-1$ then we can write (as pseudocode)

```
F=68;
P=1705;

for l=0:F-1
    v=0;
    for  p=0:P-1
        if carrier==data_carrier
            d(v,l)=u(p+l*P);
            v=v+1;
        end
    end
end
```

The PRBS is to be re-initialised at the start of every OFDM frame.

The polynomial for the PRBS generator for data carriers is

$$X^{23} + X^{18} + 1,$$

as specified by ITU-T recommendation O.151, clause 2.2.

Appendix B: Tap weight realisation using MEDS (Method of Exact Doppler Spread)

1 Overview

Although not formally part of the channel model itself, the method of generating the specified stochastic tap weights is important and has an impact when results are repeated or compared. To allow consistency, it is preferable to avoid the use of random noise generators, as their behaviour may vary between simulation platforms even if initialising seeds are specified. Instead, a quasi-stochastic tap weight may be used which is repeatable run-to-run.

An approach to obtaining such deterministic filtered noise as a basis for generating tap weights in the channel model is to approximate the Doppler spectrum using a sum of sinusoidal tones of appropriate frequencies and amplitudes. Accurate spectral shaping can be obtained without the need to define precise FIR filters with a Jakes frequency characteristic. The simulations are repeatable across computing platforms, which may not be the case if noise generators or noise seeds are being relied on.

2 Approach

The chosen ‘sum of sinusoids’ approach for the current set of simulations results is based on the MEDS model proposed by Patzold et al. [1].

We define a quasi-stochastic tap weight process in the following way:

$$u(t) = u_1(t) + ju_2(t) \quad \ldots\ldots\ldots\ldots\ldots\ldots\ldots\ldots\ldots\ldots (15)$$

With

$$u_i(t) = \sum_{n=1}^{N_i} c_{i,n} \cos(2\pi f_{i,n} t + \theta_{i,n}) \qquad i = 1,2 \quad \ldots\ldots\ldots\ldots\ldots\ldots\ldots\ldots\ldots\ldots\ldots\ldots (16)$$

and

$$c_{i,n} = \sigma_0 / \sqrt{2N_i} \quad \ldots\ldots\ldots\ldots\ldots\ldots\ldots\ldots\ldots\ldots (17)$$

$$f_{i,n} = f_{\max} \sin\left[\frac{\pi}{2N_i}\left(n-\frac{1}{2}\right)\right] \ldots\ldots\ldots\ldots\ldots\ldots\ldots\ldots\ldots\ldots (18)$$

In the NGH channel model, a stochastic process is needed for taps 2-8, and a different pair of N_1, N_2 is chosen for each of these taps, according to

$$N_1 = 18 + 2(tap\_no. - 1) \ldots\ldots\ldots\ldots\ldots\ldots\ldots\ldots\ldots\ldots (19)$$

$$N_2 = N_1 + 1 \ldots\ldots\ldots\ldots\ldots\ldots\ldots\ldots\ldots\ldots (20)$$

The initial phases, random in NGH model, are made deterministic as

$$\theta_{i,n} = \frac{n}{2N_i} \ldots\ldots\ldots\ldots\ldots\ldots\ldots\ldots\ldots\ldots (21)$$

$u(t)$ as defined provides us with the stochastic term in c_{11} of each tap.

For the other components, c_{12}, c_{21}, and c_{22} we use the equation (16) but with t replaced by

t+10 for generating c_{12}

t+20 for generating c_{21}

t+30 for generating c_{22}

This ensures a high level of decorrelation of the components of **H**.

Finally the prescribed intra-tap correlation properties can be introduced through the transition matrix $\mathbf{\Gamma}$ appropriate to the indoor or outdoor models as required.

The synthetic Jakes spectrum resulting from the above process is shown in figure 11 above, obtained by taking the Fourier transform of a typical process $u(t)$ in MATLAB.